

8 / 1979

J. Sokół-Supel, A. Sawczuk

**COMPARISON
OF THE COMPLETE LIMIT ANALYSIS
AND THE YIELD LINE
THEORY SOLUTIONS FOR PLATES**

A. An outline of experimental studies



WARSZAWA 1979

Praca wpłynęła do Redakcji dnia 6 lutego 1979 r.

Zarejestrowana pod nr 8/1979



N a p r a w a c h r ę k o p i s u

Instytut Podstawowych Problemów Techniki PAN

Nakład 150 egz. Ark. wyd. 1. Ark. druk. 1,5

Oddano do drukarni w lutym 1979 r.

Nr zamówienia 108/0/79

Warszawska Drukarnia Naukowa, Warszawa,
ul. Śniadeckich 8

Joanna Sokół-Supel, Antoni Sawczuk
Zakład Teorii Konstrukcji

COMPARISON OF THE COMPLETE LIMIT ANALYSIS AND
THE YIELD LINE THEORY SOLUTIONS FOR PLATES
A. AN OUTLINE OF EXPERIMENTAL STUDIES

1. Objectives.

For plates obeying the Johansen yield criterion the complete limit analysis solutions are available in several cases. This criterion is usually employed in the yield line theory to obtain an upper bound to the collapse load since the respective calculations concern solely the mechanism of motion under the limit load. The complete solutions coincide in many cases, however, with those furnished by the yield line theory as far as the collapse load and the mechanism of plastic motion are concerned. In many cases the complete solutions differ in comparison with those furnished by the yield line theory where the result is more over strongly influenced by the choice of collapse mechanisms to be considered. It appears advisable to make properly conceived tests concerning a case when the complete solution differs from those available from the yield line theory. The purpose of such tests is double. In the first place the aim is to verify the exact solution both as far as the collapse load and the deflection rate field are concerned. Moreover we are interested in learning about the experimental collapse mode of a reinforced plate in order to employ appropriate mechanism of plastic collapse, yielding better upper bounds via the yield line theory.

To these ends tests regarding the limit analysis of plates obeying the Johansen yield criterion are intended. Experiments are proposed on point loaded circular plates

where complete solutions differ from those already known or new furnished up to now by the yield line theory both as regards the collapse load and the collapse mode.

2. Problem formulation.

For the yield criterion of the maximum principal moment the complete solutions can easily be obtained for various cases of loading of simply supported isotropic plates. A perfectly plastic plate at the limit state is totally or partially in the parabolic, isotropic or hyperbolic stress régime either below the yield stress, whenever the respective part of the plate remains rigid [5]. The type of stress régime depends on the equation of the yield surface zone employed [2], [5].

Stress discontinuities may occur across the line separating different stress régimes, [5,6]. Discontinuities of the tangent to the deflected surface are also admissible at the maximum principal moment yield criterion. This property is used in the yield line theory to generate collapse mechanisms with hinge lines, [3], [4].

The complete solution of a limit analysis problem for a plate consists of the collapse load intensity of the associated field of moments and shear forces satisfying a) the internal equilibrium requirements, b) the prescribed stress boundary conditions, c) the displacement velocity field specifying a kinematically admissible collapse mechanism associated with positive energy dissipation at the plate collapse.

Complete solutions may differ from the results obtained employing the yield line theory both in the collapse load multiplier and in the yield pattern because of the difference in the set of equations used respectively. A yield line solution does not specify the stress field in the plate at the state of collapse as it disregards the differential equations of equilibrium, which are taken into account in any complete solution.

The tests intended should furnish an experimental evidence as regards the deformation pattern and magnitude of the collapse load. The type of loading and boundary conditions are chosen so as to allow for the complete solution to consist of parabolic and isotropic régimes. The corresponding velocity field for deflections consists then of developable surfaces of arbitrary surfaces of positive Gaussian curvature respectively. The tests thus should make possible to establish the yield mechanism and to specify its geometrical parameters

In the yield line theory any collapse mode consists of developable surfaces which, in fact, correspond to parabolic stress régimes. This is why the tests are to be made for such cases of loading and boundary conditions where the complete solution involves more than a single parabolic stress régime.

A circular simply supported plate furnishes the case when the yield line theory results differ in comparison with the complete solution. Two point loads are applied on the plate diameter. The ratio of the loads applied vary in order to allow to study both the yield pattern variation as well as the collapse load multiplier obtained from the both theories considered. The respective theoretical solutions will now be given, after the notation employed is specified.

3. Notation

R , a reference length, chosen here to be the plate radius,

$\rho = \frac{r}{R}$, the dimensionless radial variable,

A , the distance of the point of loading from the circular plate center,

$a = \frac{A}{R}$, the dimensionless distance of the point load,

M_0 , the yield moment in positive bending,

M'_0 , the yield moment in negative bending,

$$\Delta = \frac{M'_0}{M_0}$$

M_x, M_y, M_r, M_θ , bending moments

T_x, T_y, T_r, T_θ , shear forces,

$m = \frac{M}{M_0}, t = \frac{TR}{M_0}$, the dimensionless bending moments and shear forces

Q_1, Q_2 , point loads

$q_1 = \frac{Q_1}{M_0}, q_2 = \frac{Q_2}{M_0}$, the dimensionless point loads corresponding to the complete solution

$$\alpha = \frac{q_2}{q_1}, \quad 0 \leq \alpha \leq 1$$

$q = (1 + \alpha) q_1$, the dimensionless total collapse load of the plates

q_+, q_{1+} , etc, dimensionless limit load corresponding to the yield line theory solution

w , a deflection velocity

$\beta = \frac{w_2}{w_1}$, the ratio of the deflection velocities of the point of load application.

4. Complete solution

Let us consider a simply supported circular plate, loaded as shown in Fig.1a. The point loads Q_1, Q_2 are applied at the equal distance A from the plate center. The complete solution consists of the paraboloid zones $SCSO_1$ and $S'BSO_2$, joined by the isotropic régime $SO_1S'O_2$. In the isotropic zone the stress field is

$$(4.1) \quad m_x = m_y = m_r = m_\theta = 1, \quad t_x = t_y = t_r = t_\theta = 0$$

Any direction is principal and the zone carries no transverse loading. The velocity field is there arbitrary and only sub-

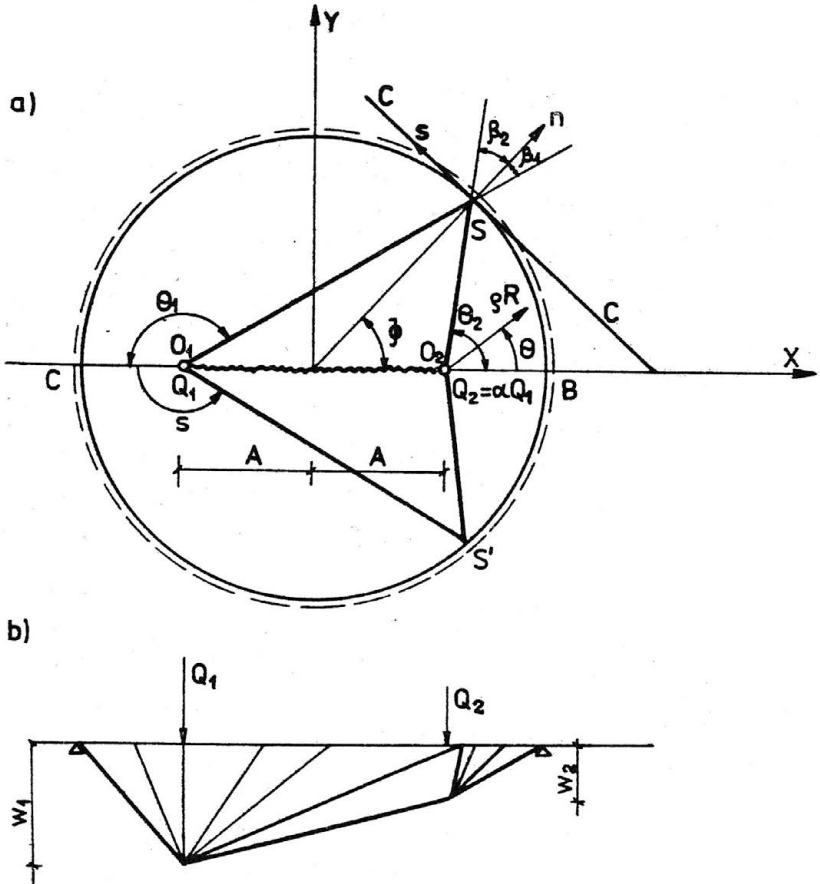


Fig. 1

jected to the condition that the Gaussian curvature of the deflected surface is non-negative there. The velocity field likely has a slope discontinuity line along the $O_1 O_2$ line.

In the parabolic zones $SCS'O_1$ and $S'BQ_2$ the bending moments and the shear forces expressed in polar coordinates with origin, each time at the point of loading, Fig. 1a,

are respectively

$$(4.2) \quad m_{\theta} = 1 \quad m_r = - \frac{\alpha^2 \sin^2 \theta}{1 - \alpha^2 \sin^2 \theta}$$

$$(4.3) \quad t_{\theta} = 0 \quad t_r = - \frac{1}{g} \cdot \frac{1}{1 - \alpha^2 \sin^2 \theta}$$

The velocity of deflection field in the parabolic zone is bounded by a developable surface. In the case of point loading considered two conical surfaces $SCS'O_1$ and $S'BSO_2$ are obtained. The vertices of the cones are at the points of load application, Fig. 1b. When fissures appear in the parabolic zones then should be oriented along the straight generators of the conical surface.

Along the lines O_1S , O_2S and symmetrically, discontinuities in the radial moment appear, as it can be seen when comparing the results (4.1) and (4.2). Between the parabolic and the isotropic régime on the lines SO_1 and SO_2 in Fig. 1a, there is a continuous transition of the circumferential derivative. The triangular part AO_1O_2 of the isotropic range rotates with respect to the axis C-C, Fig. 1a, which is tangent to the plate boundary at S. Geometrical considerations lead to the conclusion that the flat element O_1SO_2 is tangent to the cones and that the points of load application have the vertical velocities related as follows

$$(4.4) \quad \beta = \frac{w_2}{w_1} = \frac{1 - \alpha \cos \phi}{1 + \alpha \cos \phi}$$

The collapse loads are calculated considering the shear force along a circumferential trajectory, [5],[6].

$$(4.5) \quad q_{\theta} = 2 \int_0^s (-t_{\theta}) ds = 2 \int_0^{\theta_1} (-t_{\theta}) g d\theta$$

and the results are respectively

$$(4.6) \quad q_{\theta} = \frac{2}{\sqrt{1-\alpha^2}} \left[\pi - \arctan(\sqrt{1-\alpha^2}) \frac{\sin \phi}{\alpha + \cos \phi} \right]$$

$$(4.7) \quad q_2 = \frac{2}{\sqrt{1-\alpha^2}} \left[p - \arctan(\sqrt{1-\alpha^2} \frac{\sin \phi}{\alpha - \cos \phi}) \right]$$

where

$$\begin{aligned} p &= 0 && \text{if } \phi \leq \arccos \alpha \\ p &= \pi && \text{if } \phi > \arccos \alpha \end{aligned}$$

The solutions are valid for the following positions of the load application points

$$(4.8) \quad 0 \leq a \leq k \sqrt{\frac{\Lambda}{1+\Lambda}}$$

where

$$\begin{aligned} k &= \sec \theta_1, && \theta_1 < \frac{\pi}{2} \\ k &= 1 && \theta_1 \geq \frac{\pi}{2} \end{aligned}, \quad i = 1, 2$$

The angle specifying the meeting point S of two parabolic régimes is defined by the following equation

$$(4.9) \quad \alpha = \frac{p - \arctan(\sqrt{1-\alpha^2} \frac{\sin \phi}{\alpha - \cos \phi})}{\pi - \arctan(\sqrt{1-\alpha^2} \frac{\sin \phi}{\alpha + \cos \phi})}$$

In Fig. 2 this angle is specified in terms of the ratio of the loads applied. This allows to derive the shape of the central isotropic zone for the given α and the load application point a .

The deflection rates at the points of loading are not equal if the loads are not equal, $\alpha \neq 1$, and the ratio is then as given in (4.4). For definiteness the deflection rates are plotted in Fig. 3, whereas the shape of the deflected surface was indicated earlier in Fig. 1b. It is seen that for the load ratio $\alpha = 1$ for any position of loading $\beta = 1$

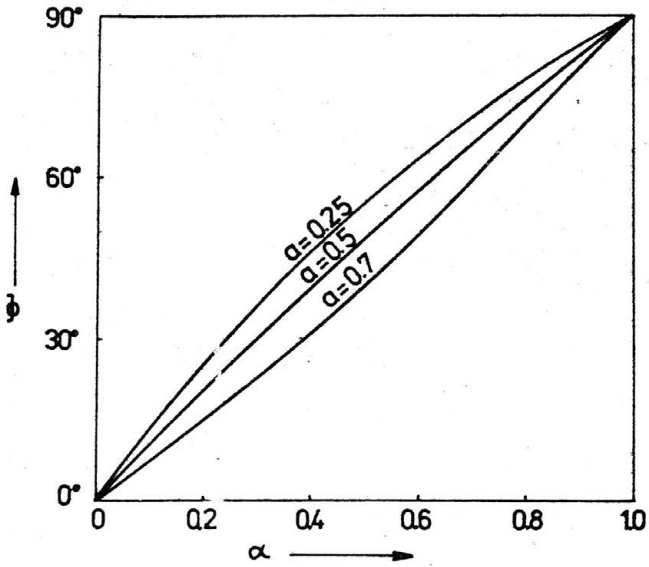


Fig. 2

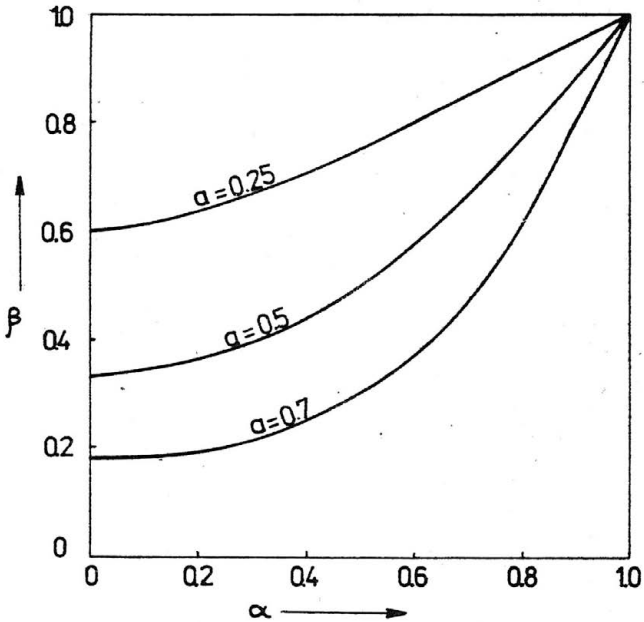


Fig. 3

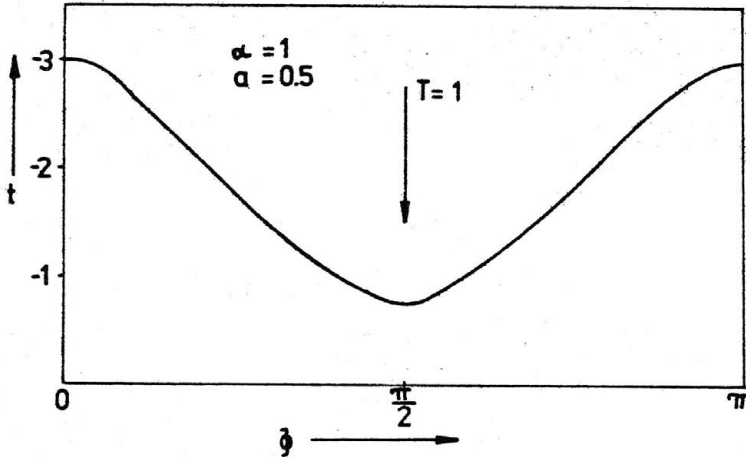


Fig. 4

It is worthwhile to mention that at the point S a concentrated reaction appears, namely

$$(4.10) \quad T = \tan \beta_1 + \tan \beta_2 = \frac{2a \sin \phi}{1 - a^2 \cos^2 \phi}$$

and the reaction on the boundary is given by the formula

$$(4.11) \quad t = t_n + \frac{\partial m_{ns}}{\partial s}$$

where m_{ns} denotes the twisting moment appearing along the simply supported edge. The moments (4.2) known the twist can easily be calculated, and hence the reaction.

In Fig. 4 the result is plotted in the case $a = 1$. The figure concerns one half of the plate and the boundary is "straightened".

5. Yield line theory solutions

To obtain a yield line theory solution regarding the load multiplier at collapse a kinematically admissible collapse mode is assumed first. For the considered plate and loading as shown in Fig. 1a let us assume first the collapse mode given in Fig. 5. The deflected surface consists here of conical elements. The zones SO_1S and $S'O_2S'$ concern cones with vertices at the points of load application whereas the zone SKS' corresponds to a cone with the vertex on the plate boundary. There is a ridge O_1O_2 on the deflected surface and it presents the intersection of cones.

In the yield line theory employing a continuous field of yield lines the dissipations of internal forces for the situations shown in Fig. 6a,b respectively is

$$(5.1) \quad D = M_0 W_0 \left\{ \int_{\theta_1}^{\theta_2} \left[1 + \left(\frac{S'}{S} \right)^2 \right] d\theta - \left[\frac{S'}{S} \right]_{\theta_1}^{\theta_2} \right\}$$

and

$$(5.2) \quad D = W_0 M_0 \left\{ \int_{\theta_1}^{\theta_2} \left[1 + \left(\frac{z'}{z} \right)^2 \right] d\theta - \left[\left(1 - \frac{z_1}{z} \right) \frac{z'}{z} \right]_{\theta_1}^{\theta_2} \right\}$$

The result concerns collapse mechanisms with conical modes [1]. The solutions (5.1) concern the cones vertices at O_1 and O_2 , whereas (5.2) gives the dissipations on the collapse mode in form of a conical surface with its vertex on

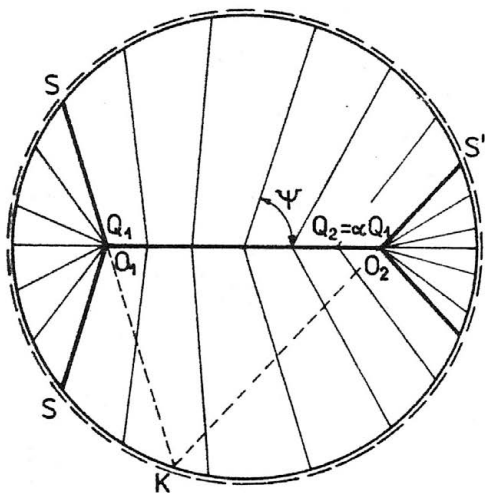


Fig. 5

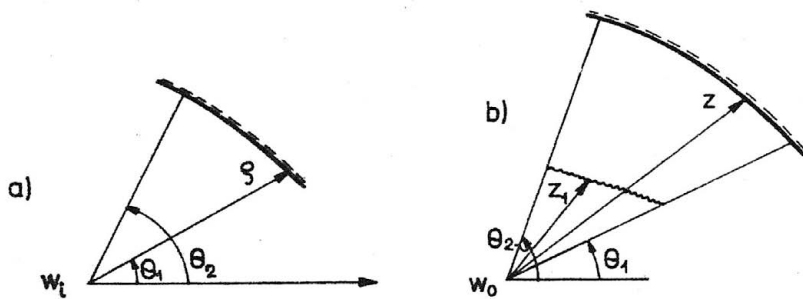


Fig. 6

the plate boundary as shown in Fig. 5.

For a given ratio α of the loads the following bound to the load carrying capacity is obtained

$$(5.3) \quad \bar{q}_+ = (1+\alpha) \min_{\psi} \frac{2}{\sqrt{1-\alpha^2} [1+\alpha \cos \psi + \alpha(1-\alpha \cos \psi)]} \cdot \left\{ (1-\alpha \cos \psi) \left(\arctan \frac{\sqrt{1-\alpha^2} \sin \psi}{\alpha + \cos \psi} \right) + \frac{4\alpha \sin \psi}{\sqrt{1-\alpha^2}} + (1+\alpha \cos \psi) \left[p + \arctan \frac{\sqrt{1-\alpha^2} \sin \psi}{\alpha - \cos \psi} \right] \right\}, 0 \leq \alpha \leq 1$$

where

$$p = 0 \quad \text{if} \quad \arccos \alpha < \psi < \frac{\pi}{2}$$

$$p = \pi \quad \text{if} \quad \psi < \arccos \alpha$$

Another collapse mode is shown in Fig. 7. Two cones are joined by the cylindrical surfaces. Calculation of the rates of internal and external dissipation eventually leads to the collapse load intensity

$$(5.4) \quad q_+ = \min_{\Omega} \frac{2(1+\alpha)}{\sqrt{1-\alpha^2}(A+\alpha B)} \left\{ \pi \cdot A + \sqrt{1-\alpha^2} \ln \left| \frac{1+\alpha \sin \Omega}{1-\alpha \sin \Omega} \right| - 2\alpha \cos \Omega \arctan (\sqrt{1-\alpha^2} \tan \Omega) \right\}$$

where $A = a \cos \Omega + \sqrt{1-\alpha^2 \sin^2 \Omega}$, $B = -a \cos \Omega + \sqrt{1-\alpha^2 \sin^2 \Omega}$

In the case when $w_1 = w_2$ and $\Omega = \frac{\pi}{2}$ the resulting collapse load is

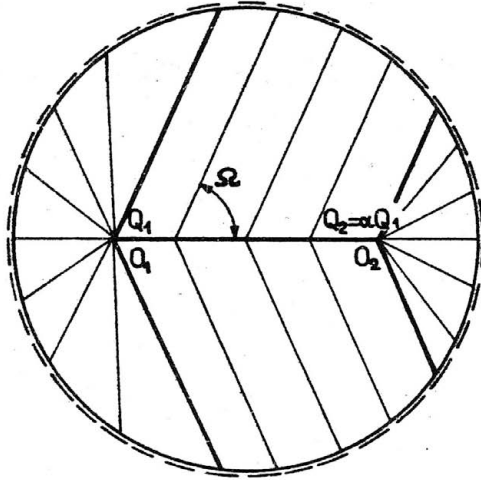


Fig. 7

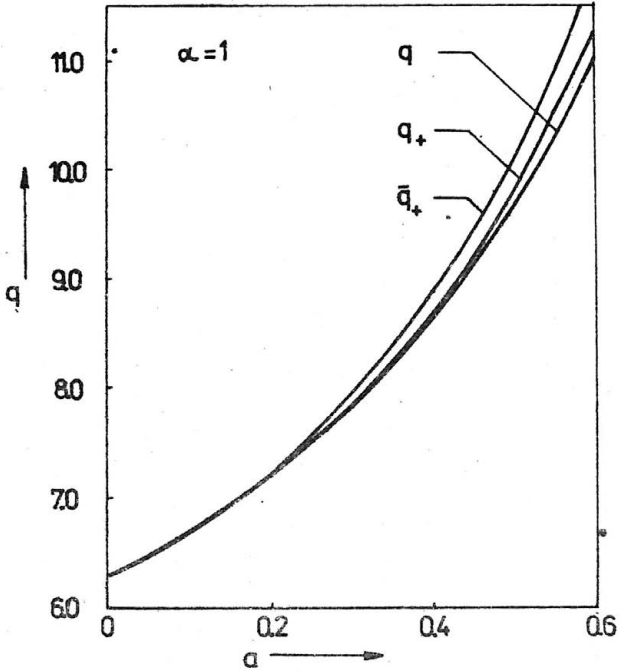


Fig. 8

$$(5.5) \quad q_+ = \frac{2}{\sqrt{1-\alpha^2}} \cdot (\pi + \ln \left| \frac{\alpha+1}{\alpha-1} \right|)$$

In Fig. 8 the collapse load intensities are shown for the two considered collapse modes. For comparison the exact result (4.4), (4.5) is shown.

6. Comparisons

Comparing the complete solution with the considered kinematical solutions one can conclude that for the load ratio $0 < \alpha < 0.5$ the differences between the solutions is of order of few per cent only. The largest differences are obtained for $\alpha = 1$ at the largest admissible excentricity for the studied complete solution involving parabolic and isotropic regimes. An illustrations of this observation is given in Fig. 9.

Thus experiments should be made at $\alpha = 1$ for $a = 0.5$ and perhaps for the value $a = 0.7$, close to the limiting case for the parabolic solution.

The considered kinematically admissible collapse modes of the yield line theory and the velocity field corresponding to the exact limit analysis solution of a rigid-perfectly plastic plate are compared in Fig. 10 at $\alpha = 1$ for the load excentricity $a = 0.5$.

Table 1 gives the respective values of the collapse load indicating the range of applicability of the complete solution presented. Similarly in Table 2 deflections rates are given for further use in the experimental analysis, when comparing the theoretical and experimental values.

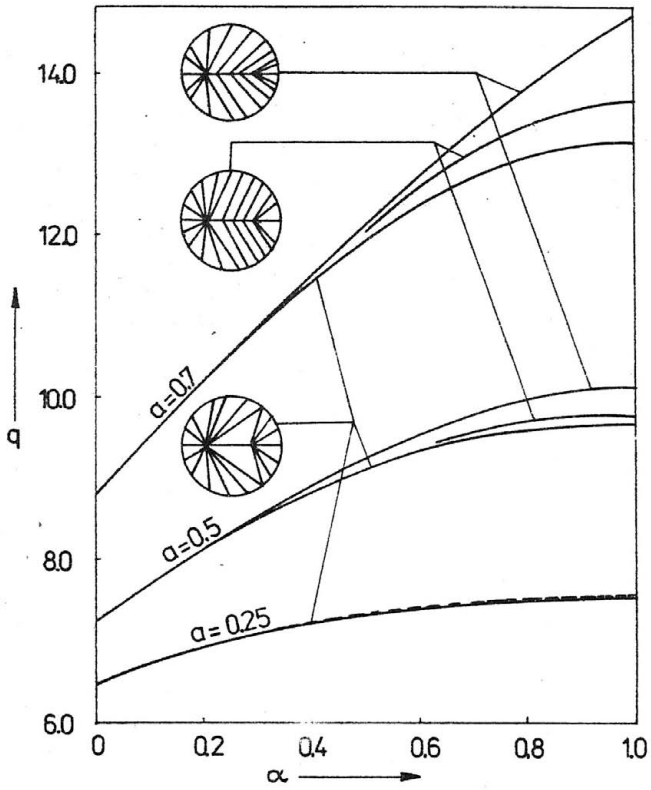


Fig. 9

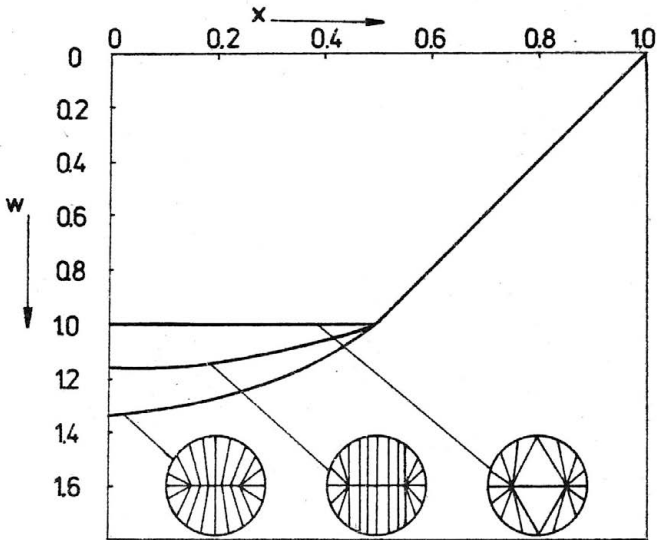








Fig. 10

Table 1

Comparison of collapse load at $\alpha=1$			
α	load carrying capacity q		
	exact	yield line theory	
		mode Fig.7	mode Fig.5
0	6.283	6.283	6.283
0.5	9.674	9.795	10.170
0.7	13.141	13.656	14.760

Table 2

Deflections rates of the loaded diameter at $\alpha = 1$												
Collapse mode	a	w/w_0										
		0	0.1	0.2	0.3	0.4	0.5	0.6	0.7	0.8	0.9	1
		0	1	0.9	0.8	0.7	0.6	0.5	0.4	0.3	0.2	0.1
  	0.5	1.0	1.0	1.0	1.0	1.0	1.0	0.8	0.6	0.4	0.2	0
		1.155	1.149	1.131	1.102	1.058	1.0	0.8	0.6	0.4	0.2	0
		1.333	1.320	1.280	1.213	1.120	1.0	0.8	0.6	0.4	0.2	0
  	0.7	1	1	1	1	1	1	1	1	0.667	0.333	0
		1.40	1.393	1.372	1.336	1.283	1.213	1.120	1	0.667	0.333	0
		1.961	1.941	1.882	1.784	1.647	1.471	1.255	1	0.667	0.333	0

7. Experiments.

The analysis of complete and kinematically admissible solutions of the considered plate problem suggests that experiments should furnish a) some information regarding the existence of an isotropic zone as well as to its extent, b) data concerning the limit load and the largest differences should appear for the load excentricity $a = 0.7$, close to the limiting case of applicability of the parabolic - isotropic solution. For $a > \sqrt{\lambda / (1 + \lambda)}$ a hyperbolic zone must appear and the exact solution is not known. In the considered case of "layered isotropy", $\lambda = 1$, the hyperbolic zone appears for $a > 0.707$.

Experiments are proposed on circular simply supported plates, reinforced uniformly on the top and bottom layer so as to obtain an isotropic plate at the yield moment ratio $\lambda = 1.0$.

Two equal point load, thus $\alpha = 1$, will be applied on the plate diameter for two excentricity ratios $a = 0.5$ and 0.7 .

The load-deflection relations will be recorded. To this end it is suggested to measure the displacements on the diameter and at the points indicated in Fig. 11.

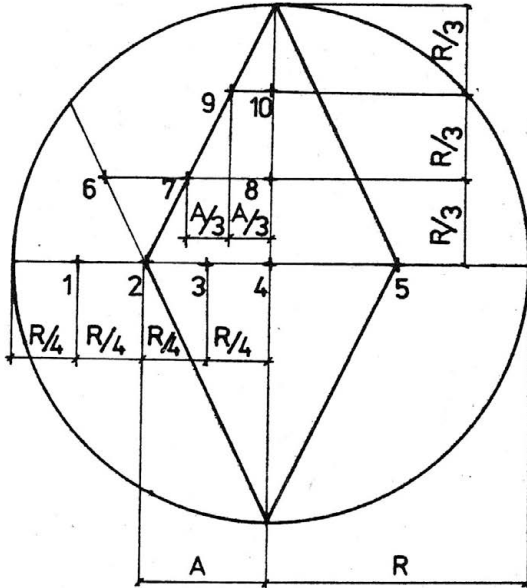


Fig. 11

The displacement gauges are placed so in order to find whether parabolic and isotropic regions can be experimentally distinguished. The data given in Table 2 can be used for comparison.

From observations of cracks and photographic recording it might be possible to get confirmation regarding presence

of an isotropic zone $SO_1S'O_2$, Fig. 1. The cracks should be there randomly oriented, contrary to the case of parabolic regimes where cracks will likely follow the generators of the developable surface of deflection rates.

It would be advisable to assess the reaction distribution along the support in order to compare the result with the theoretical previsions obtained from the complete solution. Existence of the concentrated force T at the point S , where two parabolic zones meet the isotropic region, would be worthwhile to investigate. The distribution of reaction is given in Fig. 4.

8. Concluding remark.

The solutions obtained as well as those available earlier have been used in preparation of this outline of experiments intended in order to compare the yield line theory with the theory yielding complete solutions to the limit analysis problems of plastic plates.

Acknowledgment. The work is related to the joint research task regarding application of the mechanics of plastic structures in engineering practice and operating between the Faculte Polytechnique de Mons and the Institute of Fundamental Technological Research. The solutions presented allow to consider an experimental program on comparisons between the limit analysis and the yield line theory of plates.

References

1. M. JANAS, Kinematical compatibility problems in yield line theory, Mag. Concr. Res. 19, 58, 1967, 33 -44.
2. Ch. MASSONNET, Complete solutions describing the limit state of reinforced concrete slabs, Mag. Concr. Res., 19, 58, 1967, 13 - 32.
3. M.A. SAVE, A consistent limit-analysis theory for reinforced concrete slabs, Mag. Concr. Res., 19, 58, 1967, 3 - 12.
4. M.A. SAVE, C.E. MASSONNET, Plastic analysis and design of plates, shells and disks, North-Holland-Amsterdam 1972.
5. A. SAWCZUK, P.G. HODGE, Jr., Limit analysis and yield line theory, J. Appl. Mech., 35, 1968, 357 - 362.
6. A. SAWCZUK, J. SOKOŁ-SUPEL, Bending of plates obeying maximum principal moment yield criterion, Bull. Acad. Polon. Sci., Ser. Sci. Techn., 23, 3, 1975, 141 - 150.